Chapter 6

What do the measurements tell us?

Key points

- Although annual mean PM_{10} concentrations are highest at roadside sites followed by urban background and lowest at rural sites, there is significant overlap between concentrations within adjacent site classifications. The gradient in PM_{10} between roadside, urban background and rural sites is considerably lower than that for NO_X, reflecting a greater regional background of PM_{10}.

- Colocated measurements of daily PM_{10} and $PM_{2.5}$ concentrations show that these are strongly correlated. Correlations of PM_{10} and $PM_{2.5}$ with black smoke are considerably weaker and lower in summer than winter. There is a tendency for $PM_{2.5}$ to PM_{10} ratios to increase with increasing $PM_{2.5}$ and for the ratio of coarse particles to PM_{10} to increase with mean daily windspeed, suggesting the importance of sea salt or resuspended crustal dusts.

- Current concentrations of lead at roadside and urban background sites in large conurbations are well below the limit values and objectives, whereas the concentrations of arsenic, cadmium and nickel are within the proposed EU assessment thresholds. All four metals show significant elevation adjacent to some industrial metallurgical sites.

- Several metals, most notably iron, manganese and copper show a distinct gradient in their concentration within airborne particles between roadside (highest), urban background and rural sites (lowest concentration).

- Concentrations of PAHs have declined at UK sites through the 1990s. Concentrations of benzo(a)pyrene were below the proposal EU target value of 1 ng m^{-3} in 2002 at all but one of the UK monitoring sites. Concentrations were below the UK air quality objective of 0.25 ng m^{-3} at 15 of the 19 sites for which data are available.

- Black smoke is a good indicator of primary combustion particles. The strongest correlations with PM_{10} are at sites in Northern Ireland, where domestic coal burning is still an important influence on air quality.

- Continuous measurements of elemental and organic carbon have been made at four UK sites. Mean concentrations declined from kerbside to urban background to rural sites with a stronger gradient for elemental than organic carbon. Analysis of data from the London Marylebone Road site shows diurnal profiles consistent with a substantial contribution from road traffic. Although elemental carbon is strongly correlated with the diurnal profile in heavy duty traffic, suggesting a source in diesel emissions, organic carbon is more closely related to the diurnal cycle of light duty vehicles. Analysis by wind direction again showed a strong relationship between elemental carbon and NO_X, whereas for organic carbon there is a strong correlation with the concentration of PM_{10}.

- A time series of weekly 24 h samples of PM_{10}, organic and elemental carbon at a rural site in Scotland show that the ratio of organic to elemental carbon increases substantially in the summer months, consistent with the influence of secondary organic compounds at this time of year.

- Sodium chloride derived from marine emissions is readily measurable at inland sites, its concentration relating to the distance which the air mass has travelled over the sea in the preceding 24 h.

- A mass closure model has been devised that is capable of accounting for a very high proportion of the variance in daily gravimetric $PM_{2.5}$ and PM_{10} concentrations. It contains the following components: ammonium sulphate, ammonium nitrate (in fine particles), sodium nitrate (in coarse particles), sodium chloride, elemental carbon, organic compounds, calcium (representative of sources such as construction and demolition dust), iron (representative of suspended soil and road dust and of non-exhaust traffic emissions) and bound water. The results of application of the model show a strong roadside increment in organic and elemental carbon from traffic exhaust emissions and iron-rich particles derived from non-exhaust traffic emissions.

- Although the fine fraction of particles at urban background sites is dominated by ammonium sulphate, ammonium nitrate, elemental carbon, organic compounds and bound water, the coarse fraction comprises primarily iron-rich dusts, calcium-containing dusts, sodium chloride, sodium nitrate and organic matter.

- The correlation of daily PM_{10} concentrations between two sites in Edinburgh and between two sites in Glasgow is very significant and, although lower, remains significant between Edinburgh and Glasgow, showing the importance of regional transport and regional meteorological influences on PM_{10} concentrations.

- An analysis of the data from the many sites measuring PM_{10} within London shows that those sites located away from traffic exhibited an average annual PM_{10} concentration in 2002 of 19.9 µg m^{-3}, which was 4.6 µg m^{-3} above the regional background of 16.5 µg m^{-3}. The traffic-influenced sites show an annual average PM_{10} concentration of 36.0 µg m^{-3} or 9.3 µg m^{-3}, with the regional background subtracted (all TEOM data). Regional background is a substantial proportion of the PM_{10} measured within London.

- The relatively few available data showing the concentration of PM_{10} as a function of distance from a major highway indicate a roadside elevation of about 30% above the background concentrations. Roadside increments of PM_{10}, $PM_{2.5}$ and PM_{coarse} at heavily trafficked sites in London and Birmingham show average roadside increments in PM_{10} varying between 8.7 µg m^{-3} and 15.6 µg m^{-3} (gravimetric). The roadside increment was highest on a heavily trafficked road with high buildings to one side, when the wind direction causes a recirculation of air across the road towards the sampler.
  Up to around half of the PM_{10} increment can be comprised of coarse particles, although the coarse particle increment in most cases is appreciably lower than the $PM_{2.5}$ increment.

- UK-wide maps of the spatial distribution of secondary sulphate, nitrate and ammonium show a gentle gradient from highest concentrations in the south and east of England to lowest concentrations in Northern Scotland and Northern Ireland.

- When data are normalised according to the number of sites in the network, there is very substantial month-to-month variation in the number of exceedences of 24 h average concentrations of 50 µg m^{-3}, emphasising the episodicity of PM_{10} concentrations.

- Specific components of PM_{10} also show episodicity, with nitrate showing a very high ratio of the 90th percentile concentration to the annual mean. Nitrate tends to show more episodicity than sulphate and was subject to a very large excursion in concentration in the spring of 2003.

- There are episodic contributions to PM_{10} in the UK caused by atmospheric transport of Saharan dust. This could lead to hourly excursions in PM_{10} concentration of over 200 µg m^{-3} (TEOM) with about half of the PM_{10} being in the form of fine particles. The frequency of significant Saharan dust episodes in the British Isles is one to two episodes per year.

- Concentrations of sea salt in the atmosphere also show considerable episodicity. Major episodes cross the country with a frequency of one to five times each year, generally in the autumn and winter months, causing PM_{10} excursions in excess of an hourly mean of 40 µg m^{-3} (TEOM) at coastal sites. There is a clear dependence of such events upon the strength of the wind.

- Biomass-burning fires remote from the UK can also provide a substantial source of elevated PM_{10} concentrations. During one such event in Western Russia, hourly mean PM_{10} concentrations across Northern England exceeded 100 µg m^{-3} (TEOM) and persisted for several hours.

- PM from construction activities can be a cause of short-term episodic peaks in PM_{10} concentrations. Such events tend to be rather localised and are highly dependent on current construction site activity. Annual mean concentration increments fall rapidly with distance, approaching background at about 100 m from the source.

- Correlations of PM_{10} with other traffic-generated pollutants such as NO_X, CO and benzene are strongest at roadside sites. At London Marylebone Road, concentrations of PM_{10}, $PM_{2.5}$, PM_{coarse} and particle number concentration are all higher on weekdays than on Sundays, despite there being little difference in overall traffic volume. This appears to be explained by the reduction in heavy duty traffic on Sundays.

- In addition to local effects, there are synoptic scale effects on average PM_{10} concentrations, with air masses arriving from the European continent showing a higher average concentration of PM_{10} and $PM_{2.5}$ than air masses with other origins.

- Abnormally high secondary PM concentrations in 1996 and 2003 were clearly associated with a high contribution of easterly wind directions corresponding to transport of air from the European mainland.

- An analysis of coarse and fine particle concentration data from London Marylebone Road clearly demonstrates a strong association with the volume of heavy duty traffic. Regression analysis indicates that the contribution of heavy duty vehicles is on average about 15-times greater per vehicle than for light duty vehicles. Traffic activity is responsible for by far the major part of the coarse particle concentrations at Marylebone Road.

- The activity of heavy duty traffic in causing coarse particle emissions and resuspension appears to be responsible for frequent daily mean concentrations in excess of 50 µg m^{-3} at a site in east London.

- Studies of major power stations have shown that primary PM emissions contribute typically about 0.25 µg m^{-3} to the annual mean PM_{10} concentrations. Evidence for rapid new particle formation in the plumes of coal- and oil-fired power stations is lacking.

- The investigation of the PM_{10} concentrations around Port Talbot is an illustration of how ambient monitoring, in combination with meteorological data, may be used to check on emissions, especially emissions from point sources. Such studies are a useful tool in site investigation. The technique was able to identify changes in ambient levels following the closure of furnace 5 in November 2001.

- Particle number concentrations are strongly influenced by road traffic, and concentrations at Marylebone Road far exceed those at central urban background locations. The diurnal profile of particle number concentration at urban sites follows that typical of traffic-generated pollutants.

- Measurements of particle size distributions show an elevation in concentrations for the diameter range 11–700 nm at London Marylebone Road compared to Bloomsbury, whereas over the majority of the size range concentrations at Bloomsbury well exceed those at the Harwell rural site.

- Traffic-generated particles with a diameter <20 nm are typically formed during mixing of the exhaust plume with ambient air by nucleation and condensation processes: this has a major influence on particle size distributions at roadside and urban sites.

- Particle size distribution data from Harwell show clear evidence of the formation of new particles through homogeneous nucleation processes, which is having a significant influence upon particles of <30 nm diameter. It appears that the events responsible for new particle production are favoured by the low pre-existing surface area of particles in air from relatively clean trajectory directions.

6.1 Overview of PM mass concentration data

6.1.1 Introduction

504. To give a general indication of PM_{10} concentrations throughout the UK, Figure 6.1 shows the annual average PM_{10} for 2003 at 196 sites using TEOM

Figure 6.1 Roadside, urban background and rural annual average PM_{10} TEOM concentrations in 2003.
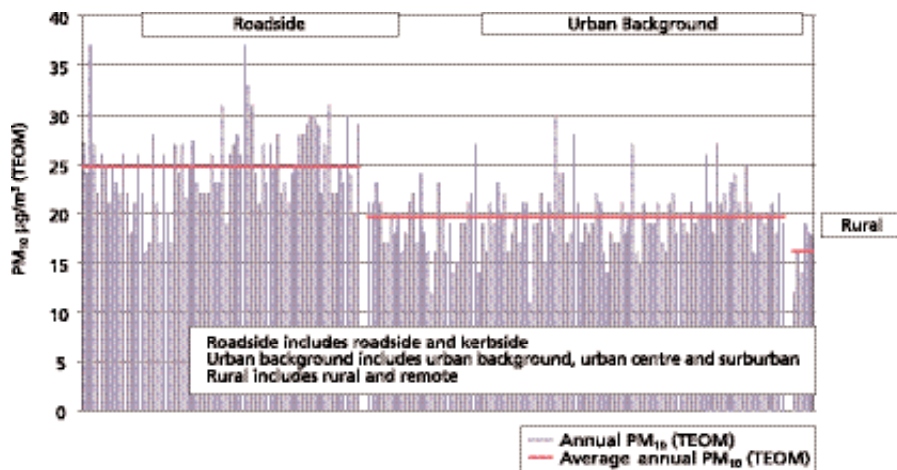
monitors, grouped into roadside, urban background and rural site locations. The average concentration for each site type is also shown. It is evident from the plot that although roadside concentrations are, on average, higher than urban background levels, which are in turn higher that rural levels, there is considerable overlap on an individual site basis. Individual site data appear in the pro forma within this report.

505. Figure 6.2 shows that, for three sample sites, the difference between PM_{10} concentrations at roadside, urban background and rural sites in much less than for NO_X.

506. At the North Kensington urban background site, NO_X concentrations are more than four-times lower than at Marylebone Road, whereas PM_{10} concentrations are less than a factor of two lower. In addition, whereas rural PM_{10} concentrations are only slightly lower than urban concentrations, NO_X concentrations are more than a factor of three lower.

507. This pattern reflects the more even distribution of PM_{10} concentrations across the whole of the UK, which arises from the wide diversity of PM_{10} sources and the contribution of secondary particulate material, as discussed in Chapter 4 and elsewhere.

Figure 6.2 Comparison of average NO_X and PM_{10} concentrations at roadside, urban background and rural sites.
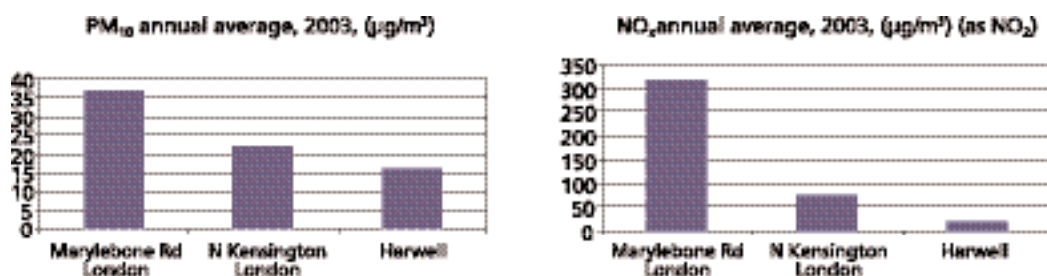
6.1.2 Relationships of PM metrics

508. Daily PM_{10}, $PM_{2.5}$ and black smoke reflectance were measured at a single location in urban background air in Edinburgh for 1 year (September 1999 to September 2000). The PM samples were collected with a manual gravimetric sampler and black smoke reflectance was converted to concentration units using the British standard reflectance calibration curve. Mean 24 h PM_{10} and $PM_{2.5}$ for the year of measurement were 15.5 and 8.5 µg m^{-3} (gravimetric). For PM_{10}, the annual mean and the 98th percentile of 33.9 µg m^{-3} (gravimetric) – approximately equivalent to the threshold for seven exceedences per year – were both within the Air Quality Strategy Objectives for Scotland. For $PM_{2.5}$, the 98th and 90th percentiles of daily means (the latter equating to 35 exceedences annually) were 21.1 and 15.3 µg m^{-3} (gravimetric), respectively. The annual mean black smoke equivalent concentration was 6.6 µg m^{-3}.

509. Figure 6.3 shows that daily concentrations of PM_{10} and $PM_{2.5}$ were strongly correlated ($r^2 = 0.75$), reinforcing the strong relationship between $PM_{2.5}$ and PM_{10} in UK urban background air, noted previously by EPAQS.

510 The distribution of daily ratios of $PM_{2.5}$:PM_{10}, black smoke:PM_{10} and black smoke:$PM_{2.5}$, divided into summer and winter, are shown in Figure 6.4. The median daily ratio of $PM_{2.5}$:PM_{10} was 0.52 (interquartile range: 0.44–0.62), showing that PM_{10} at this site is approximately equally apportioned, on average, between fine and coarse particles. The narrow interquartile range is a consequence of the strong correlation between $PM_{2.5}$ and PM_{10}. The median (and interquartile ranges) for daily ratios of black smoke:PM_{10} and black smoke:$PM_{2.5}$ were 0.42 (0.27–0.59) ($r^2 = 0.18$) and 0.80 (0.51–1.09) ($r^2 = 0.27$), respectively. The poorer correlation and much wider variability in these latter ratios reflects the fact that black smoke is a strong indicator for a specific source contributor to PM (combustion-derived dark particles), rather than being a measure of all particles.

511. Figure 6.4 also shows that daily ratios of black smoke:PM_{10} and of black smoke:$PM_{2.5}$ were significantly lower in summer than in winter, reflecting seasonal factors, particularly the higher winter concentrations of black smoke caused by poorer dispersion of emissions from ground-level sources.

512. There was a significant trend for the proportion of $PM_{2.5}$:PM_{10} to increase with increasing $PM_{2.5}$ (Figure 6.5), but less strongly with increasing PM_{10}. This indicates a trend for variations in daily PM_{10} to be driven more by variations in $PM_{2.5}$, superimposed on a more constant contribution from the coarse fraction PM_{coarse} (of ~10 µg m^{-3} (gravimetric) in these Edinburgh data).

513. The ratio of coarse particles to PM_{10} increased with mean daily windspeed (Figure 6.6), consistent with the dominant coarse component source being wind-blown or resuspended dust or sea salt.

6.1.3 Relationship between $PM_{2.5}$ and PM_{10}

514. Measurements of PM_{10} and $PM_{2.5}$ were obtained at four pairs of roadside and background sites at Elephant and Castle, High Holborn and Park Lane in London and Selly Oak in Birmingham using a manual gravimetric sampler. The data obtained at the roadside and background sites at Elephant and Castle are shown in Figures 6.7 and 6.8, respectively. Data obtained at the other sites were similar

Figure 6.3 Scatter plot of 1 year (September 1999 – September 2000) of 24 h PM_{10} and $PM_{2.5}$ in urban background air in Edinburgh.
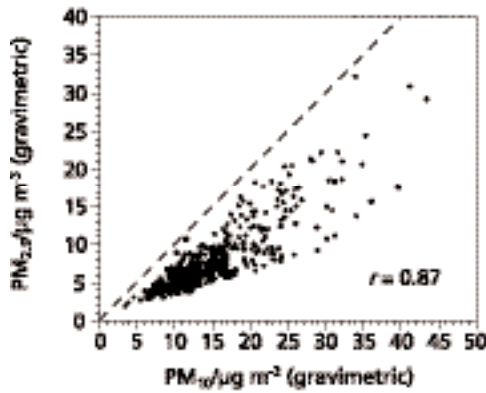

Figure 6.4 Distribution of 1 year of 24 h PM_{10}, $PM_{2.5}$ and black smoke ratios in urban background air in Edinburgh.
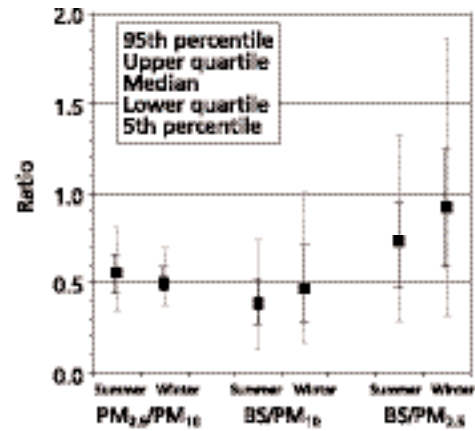

Figure 6.5 Ratio of $PM_{2.5}$: PM_{10} with $PM_{2.5}$, for 24 h measurements in urban background air in Edinburgh.
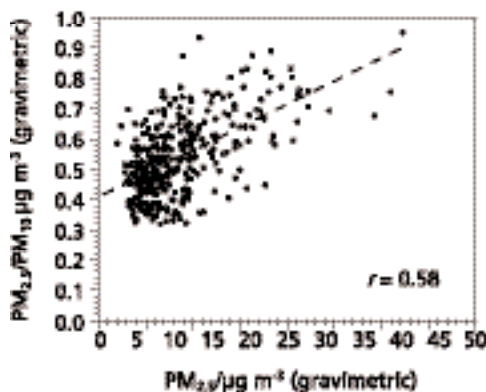

Figure 6.6 Ratio of PM_{coarse}: PM_{10} with mean windspeed for 24 h measurements in urban background air in Edinburgh.
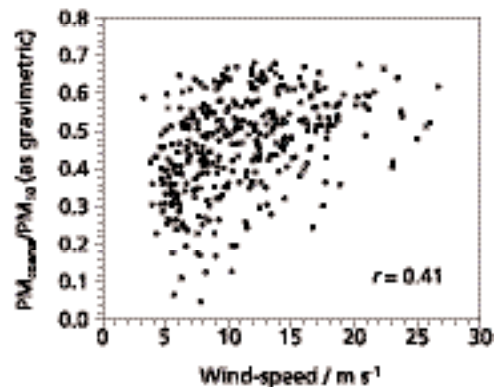

Figure 6.7 Elephant and Castle $PM_{2.5}$ versus PM_{10} roadside site.
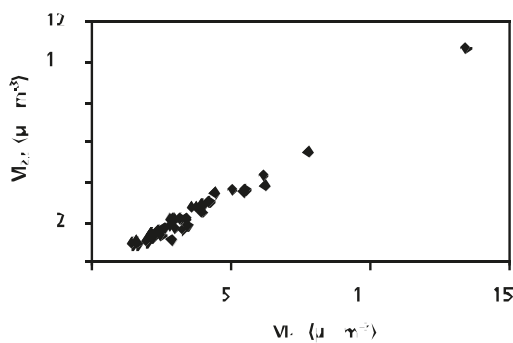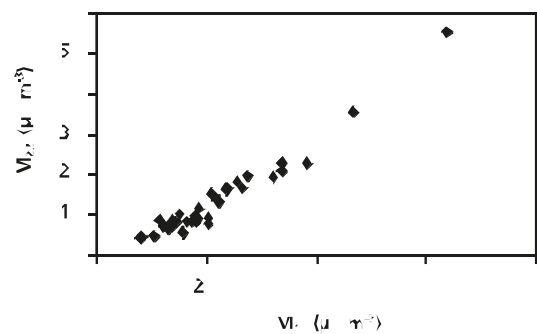

Figure 6.8 Elephant and Castle $PM_{2.5}$ versus PM_{10} background site.

to those obtained at Elephant and Castle, having a generally curvilinear form with an increasing gradient at larger values. This is consistent with the higher values of PM_{10} (and $PM_{2.5}$) being driven by episodes of high levels of $PM_{2.5}$ from distant sources.

515. The coefficients and correlation coefficients of lines fitted to the data using a reduced major axis (RMA) regression of $PM_{2.5}$ upon PM_{10} for each site are shown in Table 6.1.

Table 6.1 Linear reduced major axis regressions of $PM_{2.5}$ on PM_{10}.

Site	Site type	RMA fit to $PM_{2.5}$ versus PM_{10} ($y = PM_{2.5}$, $x = PM_{10}$)	r^2 coefficient
Elephant and Castle	Roadside	$y = 0.81\,x - 5.46$	0.97
	Background	$y = 0.87\,x - 5.31$	0.94
High Holborn	Roadside	$y = 0.83\,x - 5.94$	0.88
	Background	$y = 0.86\,x - 6.73$	0.92
Park Lane (all measurements)	Roadside	$y = 0.72\,x - 2.38$	0.96
	Background	$y = 0.86\,x - 3.97$	0.92
Selly Oak	Roadside	$y = 0.79\,x - 3.71$	0.93
	Background	$y = 0.74\,x - 2.82$	0.93

516 The most heavily trafficked roadside sites have lower values for the gradient of the $PM_{2.5}$ versus PM_{10} relationship. Conversely, the corresponding background sites also have the highest values of gradient. Lower gradients indicate a higher contribution of PM_{coarse} at the heavily trafficked sites.

517. The mean of the ratio of the PM_{coarse} increment to the $PM_{2.5}$ increment at each location is shown plotted against the traffic volume at the roadside site in Figure 6.9. Again, the evidence is of a larger proportion of PM_{coarse} at the more heavily trafficked sites. The Park Lane data are split according to wind direction.

Figure 6.9 Ratio of roadside increments versus traffic volume.
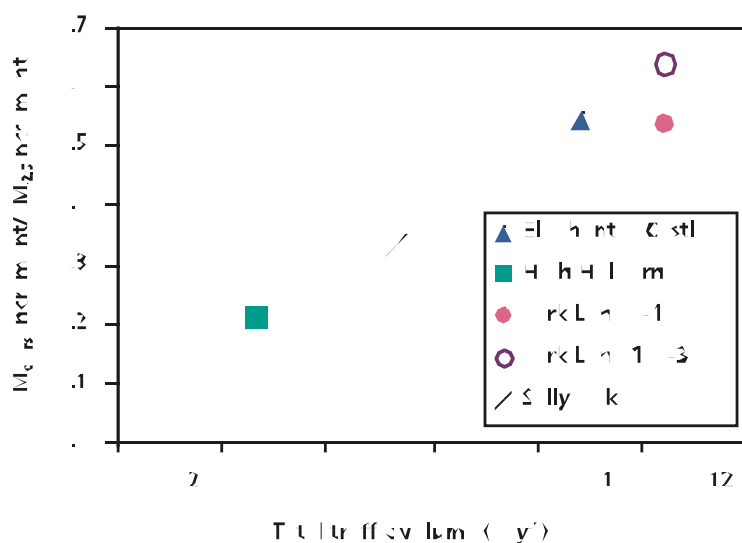
6.1.4 Specific components of airborne particles

6.1.4.1 Metals: network data

518. A description of the UK monitoring networks for heavy metals is provided in Chapter 5. A detailed analysis of trends for specific metals is given in Chapter 7. A summary of limit values, assessment thresholds and air quality objectives applicable to heavy metals appears in Table 6.2 below.

Table 6.2 EU limit values and assessment thresholds and National Air Quality Strategy Objectives for metals.

Pollutant		Concentration	Date to be achieved by
Lead	Limit value	0.5 µg m^{-3}	01/01/05
	Objective	0.5 µg m^{-3}	31/12/04
	Objective	0.25 µg m^{-3}	31/12/08
Arsenic	Assessment threshold	6 ng m^{-3}	NA
Cadmium	Assessment threshold	5 ng m^{-3}	NA
Nickel	Assessment threshold	20 ng m^{-3}	NA

519. Metal concentrations measured in 2002 within the UK multi-element network and the UK industrial network are described in Table 6.3.

520. Concentrations at roadside and urban background sites in large conurbations are well below the limit values and objectives for lead and below the proposed assessment thresholds for arsenic, cadmium and nickel. Significantly higher concentrations of iron measured at roadside sites compared with urban background sites may reflect the contribution from particle resuspension or brake wear.

521. Concentrations of arsenic, cadmium, nickel and lead are significantly higher at monitoring sites in close proximity to metal processing industries, depending upon the precise nature of the process. Although levels of lead are below both the limit value and 2004 objective, they are currently equivalent to the 2008 objective at two locations. Concentrations of cadmium and nickel exceed the proposed assessment threshold at four locations.

6.1.4.2 Metals: other data

522. A summary of the concentration of trace metals measured in PM_{10} and $PM_{2.5}$ in urban air in the UK is shown in Table 6.4.

523. The apportionment of metal between $PM_{2.5}$ and PM_{coarse} and between water-soluble and non-water-soluble fractions in these two size fractions, for the data from Edinburgh is shown in Figure 6.10. Figure 6.10b shows that the proportion of metal in PM_{10} that is contained within $PM_{2.5}$ varies widely, ranging from only 13% (titanium), 17% (iron) and 21% (nickel) to 63% (zinc), 72% (vanadium), 82% (arsenic), 84% (lead) and 95% (cadmium), on average. The proportion of each metal that was water-soluble in each size fraction also varied widely.

Table 6.3 Metal concentrations measured in the UK in 2002.

(a) Multi-element network sites.

Site name	Site type	Metal concentration (ng m^{-3})										
		As	Cd	Ni	Pb	Pt	V	Zn	Cr	Cu	Fe	Mn
London Brent	Roadside	1.7	0.9	2.9	22	0.011	3.8	34.2	7.2	24.3	810	10.7
London Cromwell Road	Roadside	1.5	0.3	4.4	27	0.009	3.8	45.7	11.8	49.2	1102	12.6
Central London	Urban background	1.9	0.4	2.2	22	0.006	3.9	35.3	4.7	21.6	598	9.2
Leeds	Urban background	1.9	0.5	2.9	43	0.006	2.8	46.2	7.8	14.3	448	11.8
Glasgow	Urban background	1.3	0.2	1.6	15	0.005	1.4	28	5.3	12.7	314	5.0
Motherwell	Urban background	1.4	0.4	1.3	13	0.006	1.2	15.1	5.2	7	224	4.1
Eskdalemuir	Rural	0.7	0.1	0.6	3	0.005	0.7	4.1	4.6	1.7	27.8	0.8

(b) Industrial network sites.

Site name	Metal concentration (ng m^{-3})			
	As	Cd	Ni	Pb
IMI, Walsall	1.9	2.2	2.1	40
BZL, Avonmouth	—	8.3	—	—
BZL, Hallan	4.8	13.1	2.0	250
Corus, Rotherham	2.7	—	—	—
INCO, Swansea	—	—	28.9	—
CEM, West Bromwich	1.7	0.7	—	—
Walkers Galvanizing, Walsall	1.6	—	—	—
White Rose, Leeds	1.7	—	3.1	—
Bruhl, Sandwell	2.5	—	—	—
Sidney Smith, Stourbridge	2.0	1.2	—	—
Britannia, Wakefield	—	—	—	250
Avesta, Rotherham	2.4	0.9	16.2	50
Brookside Metals, Willenhall	1.8	5.1	2.0	190
Elswick, Newcastle	1.7	3.7	1.9	160

Table 6.4 Comparison of total metal concentrations in urban PM samples from the UK. (The years denote the period during which samples were collected.)

Component (ng m^{-3})	PM$_{10}$			TSP			PM$_{2.5}$	
	Edinburgh 1999–2000[a]	Birmingham 2000–2001[b]	Birmingham 1992[c]	Glasgow 2000[d]	London 1999[d]	Liverpool 1994–1996[e]	Edinburgh 1999–2000[a]	Birmingham 1992[c]
Ti	3.7	—	16.6	—	—	—	0.4	11.9
V	1.1	—	7.4	1.7	4	7.3	0.7	2.4
Cr	1.6	—	12.6	8.9	2	2.1	0.5	6.2
Mn	2.9	6.4	16.3	6.9	12	8.4	0.7	64
Fe	183	204	301	399	870	340	27.6	187
Ni	3.4	2.5	4.8	4.8	5	3.0	1.0	1.9
Cu	4.9	12.0	38.7	12	21	21	1.4	8.5
Zn	13.3	29.9	353	30	41	36	7.5	55.6
As	0.4	—	5.7	—	—	—	0.30	1.5
Cd	0.34	0.51	—	0.4	—	—	0.4	—
Pb	14.1	27.4	91	—	—	43	13.6	17.1

[a]Median value ($n = 366$), urban background air, analysis by acid-digest and ICP-MS (Heal *et al.*, 2004). [b]Mean value ($n = 30$), roadside, analysis by acid-digest and ICP-MS (Harrison *et al.*, 2003). [c]Mean value ($n = 55$), analysis by PIXE (Harrison *et al.*, 2000). [d]Mean value ($n = 12$), analysis by XRF and INAA (DEFRA, 2003a). [e]Geometric mean value ($n = 60$), analysis by ICP-MS (Chester *et al.*, 2000).

For example, the proportion of water-soluble titanium and iron was ≤10% in both PM$_{2.5}$ and PM$_{coarse}$, whereas ≤74% of vanadium, zinc and lead in PM$_{2.5}$ was water-soluble. For the PM$_{10}$ fraction as a whole, >50% of the metal was water-soluble for vanadium, zinc, arsenic and cadmium. For all 11 metals quantified, a greater proportion of metal was water soluble in the fine fraction than in the coarse fraction.

524. On average, for the data from Edinburgh, the 11 trace metals constituted 1.8% of daily PM$_{10}$ mass (maximum daily proportion 9.0%) and 0.8% of daily PM$_{2.5}$ mass. The PM$_{coarse}$ fraction of PM$_{10}$ was, therefore, almost a factor of four more enriched with these metals (median daily value 3.1%) than the PM$_{2.5}$ fraction. These proportions varied significantly with season, with coarse particles being more enriched with trace metal in summer and vice versa for fine particles. A greater proportion of the trace metal in PM$_{2.5}$ (~30%) was water-soluble than in PM$_{10}$ (~15%).

525. Although iron is the dominant trace metal, its relative contribution to the sum of the measured trace metal concentration varies widely with both size and water-soluble fractions (Figure 6.11). The contributions of total iron to the sum of total metal for the 11 trace metals measured in PM$_{10}$, PM$_{2.5}$ and PM$_{coarse}$ are 80%, 51% and 89%, respectively, whereas the contributions of water soluble iron to the sum of water-soluble metal are only 43%, 19% and 64%, respectively. In fact, within PM$_{2.5}$, the amount of water-soluble lead and zinc both exceed that of iron. Across all the particle size fractions, over 90% of the water soluble or total mass of metals analysed is always contributed by iron, copper, zinc and lead. Titanium, vanadium, chromium, manganese, nickel, arsenic and cadmium each only constitute <2%, on average, of the total metal measured in each size fraction. The greater water solubilities of vanadium and manganese mean these two metals are relatively more important contributors to water soluble metal, although both still constitute <5% each (Figure 6.11).

526. A comparison of the proportion of trace metal in 24-h samples of PM$_{10}$ from six sites across the UK is shown in Figure 6.12. The values of total PM$_{10}$ (TEOM) concentrations are shown in the first column of the figure. The main feature of the data is for the proportion of most of the trace metals in PM$_{10}$ to be roughly comparable across the sites measured (even though the total airborne concentration of each metal will vary with total mass concentration of PM$_{10}$). There are some minor exceptions, presumably indicating enhanced local sources of a particular element at a particular receptor. For example, copper is relatively more abundant in PM$_{10}$ at the Marylebone Road location and is relatively less abundant as size of urban area decreases; zinc is more abundant in Birmingham, but this can be attributed to local industrial point sources; vanadium is relatively more abundant in Belfast.

6.1.4.3   PAHs

527. Chapter 5 outlines the network for PAH monitoring in the UK and the method of measurement. A total of 32 PAH species are measured at some or all of the 25 monitoring locations currently in operation. However, this brief analysis of the data will concentrate on the compound benzo[a]pyrene. EPAQS has recommended setting a national standard for PAHs using annual average

Figure 6.10 Median concentrations of trace metals in one year of 24-h samples of PM_{10} in background air in Edinburgh, subdivided into $PM_{2.5}$ and PM_{coarse} and further subdivided into water-soluble and non-water-soluble metal. (a) Absolute concentrations and (b) relative proportions.
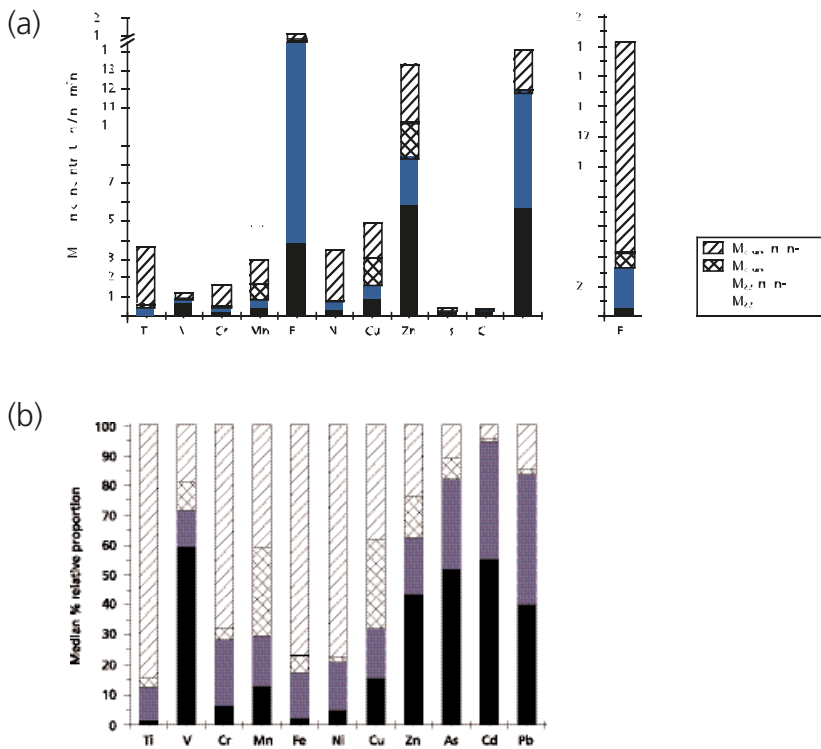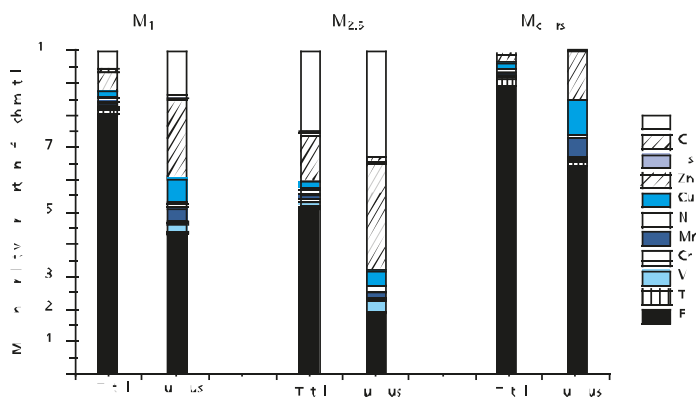

Figure 6.11 Relative contribution of each metal to the sum of 11 trace metals measured in PM_{10}, $PM_{2.5}$ and PM_{coarse} in background air in Edinburgh both water-soluble and total metal. (Data are median values of n = 366 daily samples.)

concentrations of benzo[a]pyrene as a marker for the human health effects of PAHs. EPAQS has recommended an annual average concentration of 0.25 ng m^{-3} as a guideline. The current draft proposal for the 4th EU Daughter Directive proposes an assessment threshold for benzo[a]pyrene of 1 ng m^{-3}.

528. Emissions of benzo[a]pyrene in the UK calculated within the NAEI show that there has been a reduction in emissions from just under 70 t in 1990 to under 10 t in 2001. In 2001 the two largest sources, accounting for about 65% of total emissions, were residential sources and other sources (mainly natural sources).

Figure 6.12 Proportion of metal (ng µg–1) in 24-h samples of PM_{10} from six sites in the UK. Although all samples are from the period September 1999–September 2000, the data presented are not all entirely concurrent.
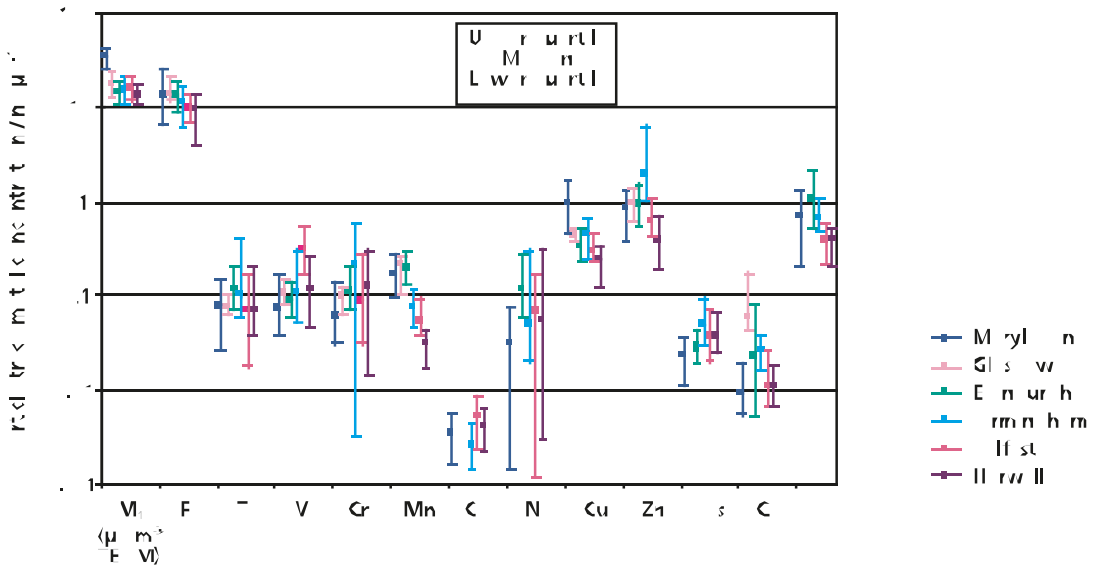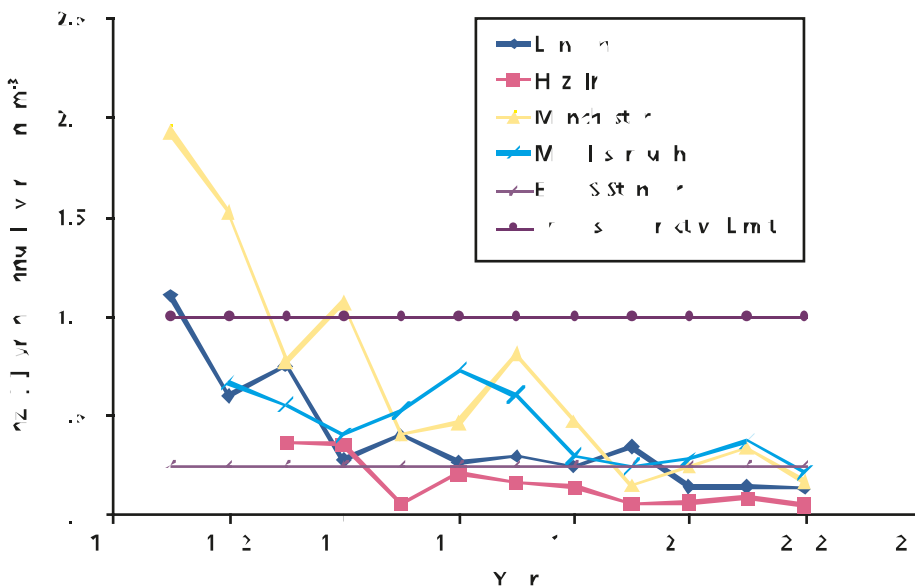

Figure 6.13 Annual average benzo[a]pyrene concentrations at four long-running sites in the UK.

529. Annual average concentrations of benzo[a]pyrene at the four long-running sites show a similar downward trend (Figure 6.13). Concentrations at the urban sites – London and Manchester – have decreased considerably and more than at the industrial site in Middlesbrough and the rural site at Hazelrigg in Lancashire.

530. **Figure 6.13** also indicates the EPAQS standard value of 0.25 ng m^{-3} and the proposed EU target value of 1 ng m^{-3}. Table 6.5 gives a summary of the benzo[a]pyrene annual average concentrations at all sites for 2000–2002. It shows that concentrations at all except one site are below the EU target value, but that the EPAQS standard was equalled or exceeded at four sites in 2002.

Table 6.5 Summary of annual mean benzo[a]pyrene concentration at all sites 2000–2002.

Site	Mean annual benzo[a]pyrene concentration (ng/m^3)		
	2000	**2001**	**2002**
Ashington	0.17	0.2	NA[a]
Belfast	—	**0.37**	0.13
Birmingham	—	0.16	0.13
Bolsover	**0.25**	**0.28**	0.24
Bromley	—	—	**0.25**
Glasgow	0.12	0.12	0.12
Hazelrigg	0.06	0.083	0.048
High Muffles	0.04	0.05	0.043
Holyhead	0.11	0.15	NA[b]
Kinlochleven	**2.3**	**0.34**	**0.38**
Leeds	—	0.16	0.18
Lisburn	**0.93**	**0.96**	**0.66**
London 2a	<0.14	0.14	0.13
Manchester	0.24	**0.34**	0.17
Middlesbrough	**0.28**	**0.37**	0.21
Newcastle	—	0.11	0.12
Newport	**0.35**	**0.36**	0.19
Port Talbot	**0.59**	**0.4**	**0.34**
Scunthorpe	1.2	**0.34**	1.4
Speke	—	—	0.14
Stoke Ferry	0.087	0.09	0.083

Note: Concentrations in bold are at or above the EPAQS recommended annual average of 0.25 ng m^{-3}.
[a]Not available due to loss of samples during analysis. [b]Sampling not undertaken in quarter 2 of 2002 due to health and safety concerns.

531. More detailed analyses of benzo[a]pyrene concentrations up to 2000 are available elsewhere (Coleman *et al*., 2001). An assessment of benzo[a]pyrene atmospheric concentrations in the UK to support the establishment of a national PAH objective (AEAT/ENV/R/0620 August 2001) are available at www.airquality.co.uk.

6.1.4.4 Black smoke

532. The black smoke method measures the reflectance of particles collected on a filter and is a measure of the elemental carbon content of the particles, which arises mainly from coal and oil combustion and automotive diesel emissions. Measurements of black smoke have been used previously as an indicator for primary combustion PM_{10} particles using the APEG receptor model (APEG, 1999). More recent analyses using this model, such as those presented in Chapter 8, have used measured NO_X concentrations in preference to black smoke. This is

because NO_X measurements are much more commonly colocated with PM measurements compared to black smoke measurements. The precision of the black smoke method is also less good at very low concentrations (see Chapter 5).

533. Black smoke measurements can, however, still be useful indicators of PM mass concentrations in areas where high concentrations are strongly influenced by domestic coal burning. Table 6.6 lists PM_{10} and black smoke monitoring sites in the UK that are either collocated or less than 1000 m apart. Mean concentrations of PM_{10}, black smoke and rural sulphate for available data between January 2001 and March 2003 are also listed in the Table 6.6 along with the intercept and regression coefficients from the APEG receptor model. Rural sulphate concentrations have been taken from the nearest site.

534. Strabane Spring Hill Park is the site with the highest measured concentrations of both black smoke and PM_{10} and the highest correlation coefficient. This suggests that black smoke is a good indicator of primary combustion PM_{10} from domestic coal burning at this site. This site also has a higher black smoke regression coefficient, suggesting that the particles are less dark in colour than at many of the other sites examined. The receptor model results suggest that primary combustion PM contributed 55% of the total PM_{10} mass at this site. Note, however, that PM_{10} measurements at this site were carried out using a ß-attenuation monitor; all other sites used TEOM.

535. The values of the intercept and regression coefficients are generally as expected, but the correlation coefficient is only >0.5 at 5 of the 15 sites examined. This suggests that the combination of black smoke and sulphate measurements are relatively poor indicators of PM_{10} concentration at many of the sites. The correlation coefficients are low and intercepts high at the Glasgow and Wigan Leigh sites. The black smoke coefficient is unusually high at the Wrexham site, where the PM_{10} monitoring site is at the roadside.

536. Figures 6.14 and 6.15 illustrate the better agreement between the PM_{10} and black smoke monitoring data at Strabane Spring Hill Park than in Belfast.

6.1.4.5 *Elemental and organic carbon*
537. Measurements of elemental and organic carbon within PM_{10} were made at Marylebone Road, North Kensington, Belfast and Harwell during 2002 and 2003 using a Rupprecht & Patashnick Series 5400 ambient carbon particulate monitor. Measurements were made for 3-h periods.

538. The mean values of elemental and organic carbon and PM_{10} for each site are given in Table 6.7. Substantially higher concentrations of elemental and organic carbon and PM_{10} were observed at Marylebone Road (a kerbside site within a street canyon) than at the other sites. The ranking of the sites was the same for organic carbon and PM_{10} but in the case of elemental carbon higher concentrations were observed at the urban centre site (Belfast) than at the urban background site (North Kensington).

Table 6.6 PM_{10} and black smoke measurements by monitors colocated within 1000 m from January 2001 to March 2003. (Statistical data from the APEG receptor model are shown.)

PM_{10} monitoring site	Black smoke monitoring site	Distance between PM_{10} and black smoke monitors (m)	PM_{10} mean ($\mu g\ m^{-3}$)	Black smoke mean ($\mu g\ m^{-3}$)	Sulphate mean ($\mu g\ m^{-3}$)	Number of Observations	r^2	Intercept	Black smoke coefficient	Sulphate coefficient
Strabane Springhill Park (BAM)	Strabane 2	Colocated	40	26	1.1	151	0.86	11.22	0.86	6.36
Nottingham centre	Nottingham 20	320	20	9	2.2	274	0.68	8.98	0.89	1.44
Newcastle centre	Newcastle 27	400	13	8	1.4	710	0.61	6.74	0.41	2.63
Newry Monaghan Row	Newry 3	Colocated	21	7	1.2	489	0.58	12.41	0.58	3.78
Bradford centre	Bradford 6	360	20	12	1.8	570	0.54	9.31	0.48	2.85
Wrexham (roadside)	Wrexham 10	540	23	4	1.9	200	0.49	9.79	2.41	2.37
Edinburgh centre	Edinburgh 25	810	20	11	1.3	365	0.44	9.26	0.66	2.94
Leicester centre	Leicester 19	920	17	15	2.2	268	0.37	7.64	0.30	2.31
Bolton	Bolton 24	860	16	8	1.8	540	0.35	7.71	0.44	2.36
Stoke centre	Stoke-on-Trent 20	860	16	10	1.8	509	0.35	7.71	0.44	2.36
Belfast centre	Belfast 45	990	19	7	1.2	591	0.34	10.60	0.41	4.26
Manchester Piccadilly	Manchester 11	540	25	14	1.8	672	0.27	13.07	0.60	2.21
Wigan Leigh	Leigh 4	Colocated	18	2	1.9	574	0.19	13.40	0.29	2.29
Glasgow kerbside	Glasgow 20	810	24	5	1.6	201	0.18	16.17	0.38	3.84
Glasgow centre	Glasgow 20	630	18	5	1.6	200	0.17	12.66	0.13	2.86

Figure 6.14 Daily means of black smoke and PM$_{10}$ (Strabane 2 versus Strabane Springhill Park).
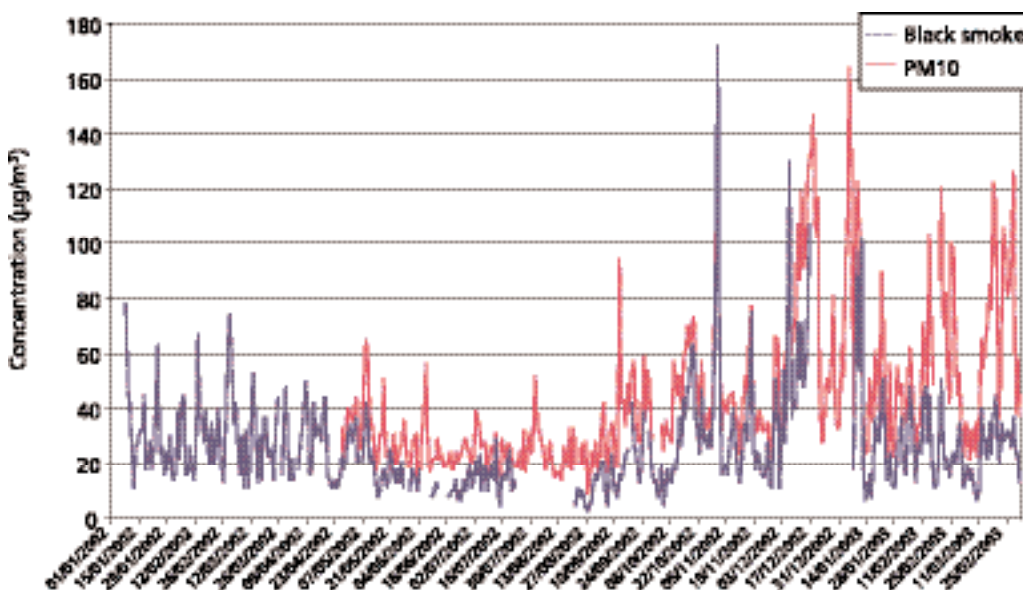

Figure 6.15 Daily mean black smoke and PM$_{10}$ (Belfast 45 versus Belfast centre).
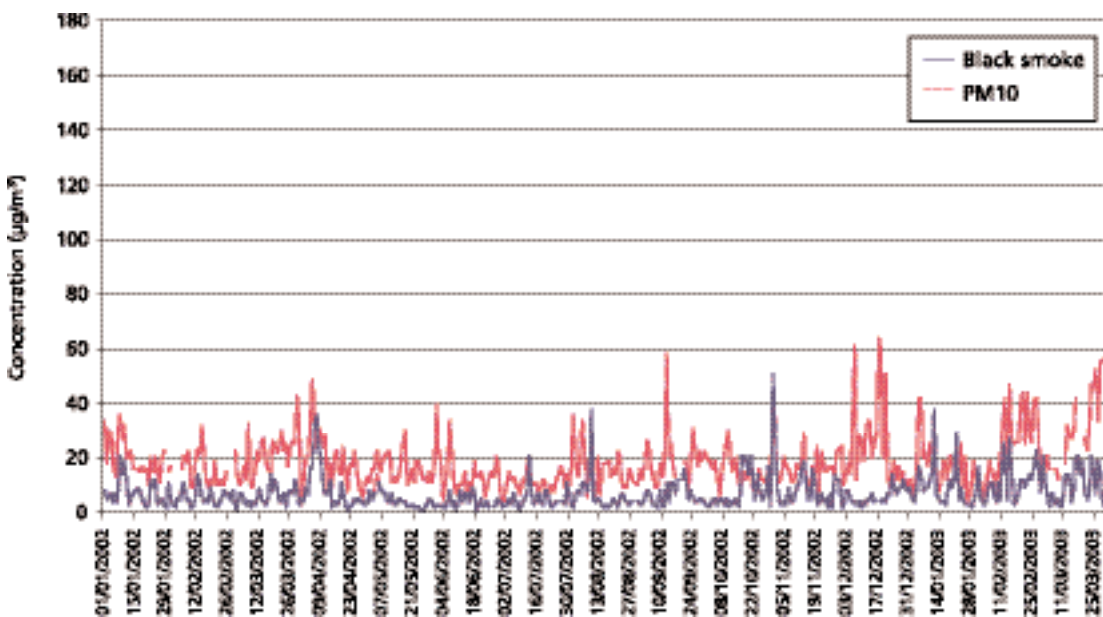

Table 6.7 Mean concentrations (and standard errors) of elemental and organic carbon and PM$_{10}$, measured at each of the four sites.

Site	Type of site	Elemental carbon (µg m^{-3})	Organic carbon (µg m^{-3})	PM$_{10}$ (µg m^{-3})
Marylebone Road	Kerbside	3.66 (0.04)	4.63 (0.03)	37.22 (0.30)
North Kensington	Urban background	0.98 (0.05)	2.45 (0.08)	24.69 (0.71)
Belfast	Urban centre	1.18 (0.03)	2.19 (0.03)	17.61 (0.23)
Harwell	Rural	0.66 (0.04)	1.94 (0.05)	13.43 (0.16)

539. The seasonal diurnal profiles of elemental and organic carbon concentrations obtained at Marylebone Road and Belfast are shown in Figures 6.16 and 6.17, respectively. No winter data were available for Belfast and due to instrumentation problems the autumn data for Marylebone Road were only available on alternate sampling periods. At both sites, minimum concentrations occurred during the 03:00 h to 06:00 h sampling period, with higher concentrations during the afternoon. At Belfast, higher concentrations of both elemental and organic carbon were seen in the evening during the autumn – possibly a result of domestic space heating.

Figure 6.16 Marylebone Road – seasonal diurnal profiles of elemental and organic carbon. (The error bars show standard error in the mean.)
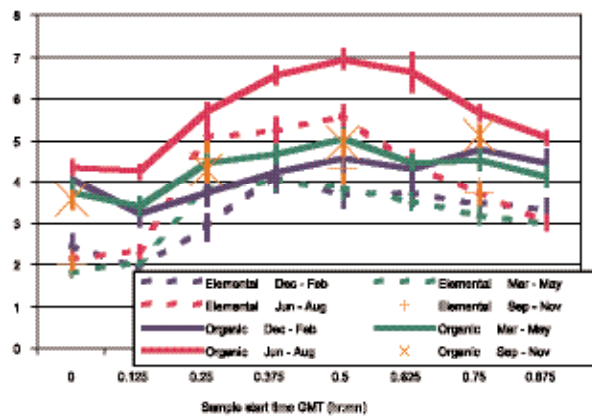
Figure 6.17 Belfast – seasonal diurnal profiles of elemental and organic carbon. (The error bars show standard error in the mean.)
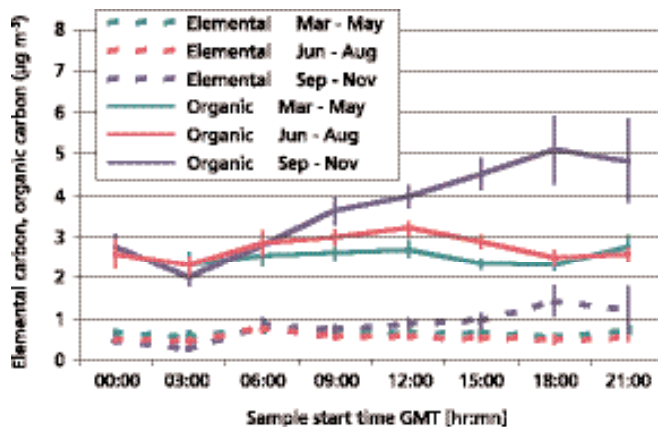
540. The normalised diurnal profiles of elemental and organic carbon at Marylebone Road are shown in Figure 6.18. A much more rapid increase in concentration at the start of the working day was apparent in the case of elemental carbon, with a more rapid decline in the evening than occurs for organic carbon. The trends in elemental and organic carbon diurnal profiles show some similarity with the diurnal profiles of heavy duty and light duty traffic volumes, respectively (Figure 6.19).

541. Variation in the normalised concentrations of elemental and organic carbon and PM_{10} with wind direction at Harwell is shown in Figure 6.20. Wind direction was measured at Benson airfield, some 25 km to the north-northeast. The profiles of the different parameters are similar except for peaks in elemental carbon at 70°

Figure 6.18 Marylebone Road 2003 – normalised diurnal profiles of elemental and organic carbon. (The error bars show the standard error in the mean.)
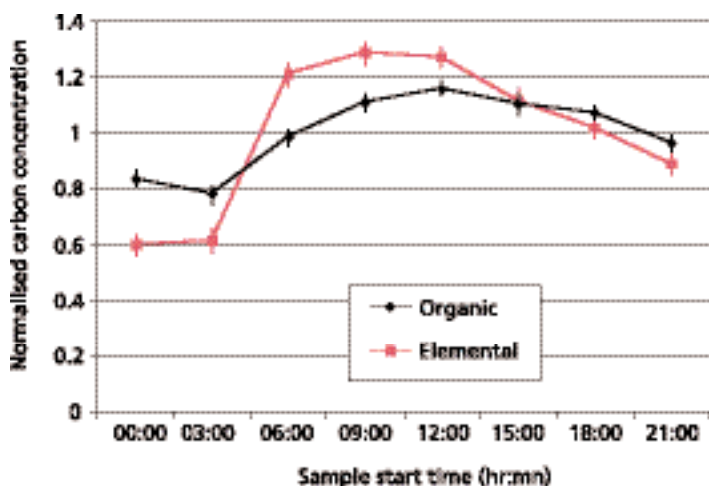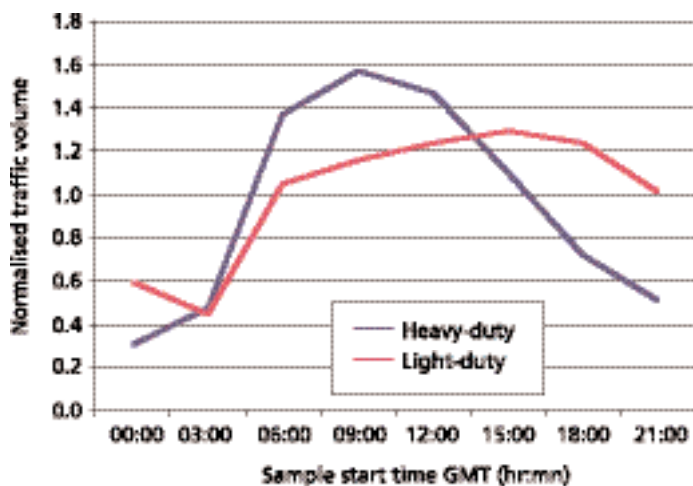

Figure 6.19 Marylebone Road – diurnal traffic profile (July 1998 to December 2001).

and 130° and at 130° in organic carbon. Observations on site identified these as the directions of local construction sites where the exhaust from site equipment was presumably the cause of the increased concentrations of carbon.

542. The corresponding plot of elemental and organic carbon and PM_{10} against wind direction for Marylebone Road is shown in Figure 6.21. Although there is a strong similarity between the profiles for organic carbon and PM_{10} (with the exception of a small peak in the PM_{10} around 90°), the profile for elemental carbon is significantly different. The profiles of organic carbon and PM_{10} are generally symmetrical about 170° wind direction with similar higher concentrations when the wind is from a range of southerly directions. These results are consistent with the cross street component of wind direction being reversed at street level in the street canyon. This carries material from vehicles onto the sampling station, which is on the southern side of Marylebone Road and is aligned approximately 80–260°.

Figure 6.20 Harwell – comparison of elemental and organic carbon and PM$_{10}$ with wind direction.
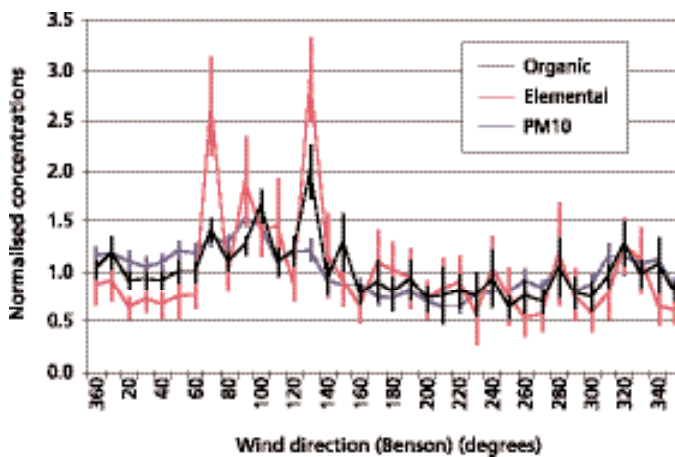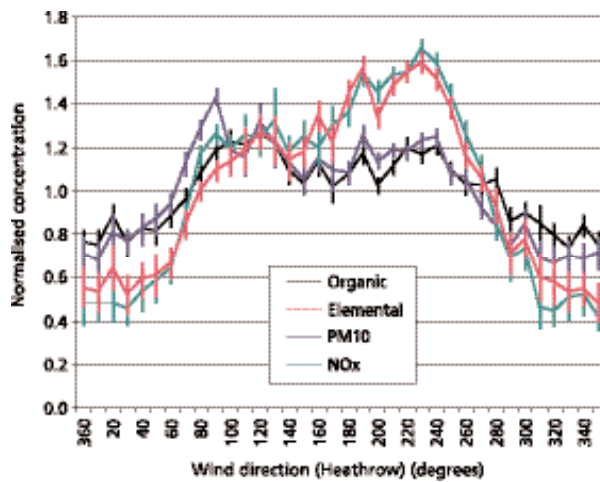

Figure 6.21 Marylebone Road – comparison of elemental and organic carbon, PM$_{10}$ and NO$_X$ with wind direction.

543. The normalised concentrations of elemental and organic carbon and NO$_X$ are also plotted against wind direction in Figure 6.21. The similarity between the profiles of elemental carbon and NO$_X$ is notable – although (as with organic carbon and PM$_{10}$) concentrations are higher when the wind is from a southerly direction, the highest concentrations occur in southwesterly winds. Other pollutants measured at Marylebone Road follow these two basic profiles of normalised concentration with wind direction. The profile of PM$_{2.5}$ follows those of organic carbon and PM$_{10}$, whereas the profiles of particle number and carbon monoxide follow the elemental carbon and NO$_X$ profiles.

544. Monitoring of traffic speeds on Marylebone Road shows a much larger reduction in speed during periods of higher traffic volume in the westbound traffic than occurs in the eastbound traffic. This may be ascribed to the presence of a pedestrian light-controlled crossing within 100 m or a major light-controlled junction 300 m to the west of the sampling site, causing the westbound flow of traffic to come to a halt. The variable length queues for these features, which may at some times stretch to the east of the sampling point, will provide an additional source of exhaust-generated material, with greater quantities being detected when the wind direction has a westerly component.

Figure 6.22 Weekly 24-h values of PM$_{10}$, organic and elemental carbon and organic:elemental carbon ratio, Bush Estate.
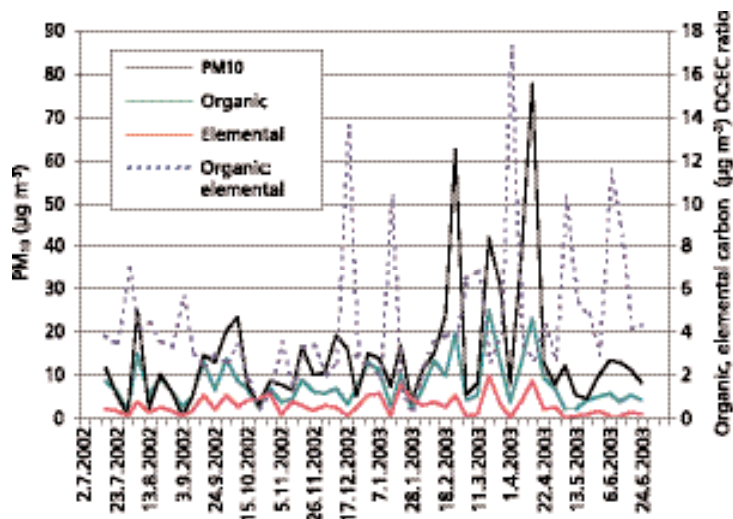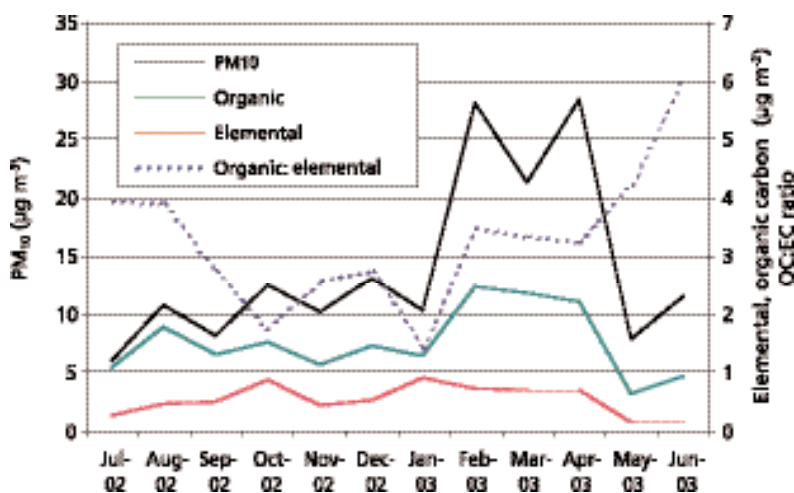

Figure 6.23 Monthly values of PM$_{10}$, organic and elemental carbon and organic:elemental carbon ratio, Bush Estate.

545. Weekly 24-h samples of PM$_{10}$, organic and elemental carbon have been collected at a rural site at Bush Estate in southern Scotland (EMP/CCC, 2004). The weekly samples appear in Figure 6.22 and as monthly means in Figure 6.23. The latter clearly shows an increased organic to elemental carbon ratio in the summer months, attributable to a higher proportion of secondary organic carbon at this time of the year. To convert organic carbon concentrations to the mass of organic matter, a factor of 1.4 is typically used.

6.1.4.6 *Airborne chloride measurements at inland sites*

546. During the measurement of the chemical components of airborne particulate over 24-h periods at three pairs of roadside and background sites in London and one pair of sites in Birmingham, it was observed that the chloride ion concentration tended to be higher when the sulphate and nitrate ion concentrations were low and vice versa. There were no significant differences between the mass of chloride at the roadside and background sites.

547. Air mass trajectories at the 950 mb level (obtained from British Atmospheric Data Centre), with end times at the middle of the sampling period, were used to calculate the distance over sea that the air mass had travelled during the previous 24 h. A simplified Western European coastline was assumed for this purpose. The assumed coastline, and examples of the 24-h trajectories of maritime and continental air masses, are shown in Figure 6.24.

548. The mass of chloride is plotted against the distance travelled over sea in the previous 24 h is shown in Figure 6.25. The distance travelled over sea in the previous 24 h is equivalent to the speed of the air over the sea multiplied by the proportion of that period spent over the sea. Although the data are scattered there is a clear trend of increasing chloride concentration with increasing distance travelled over the sea. The use of a 24-h trajectory to calculate distance over the sea gave a better correlation than other time periods. The equations for plots of chloride concentration against distance over sea for various periods fitted by least squares are presented in Table 6.8.

Table 6.8 Relationship of chloride concentration ($\mu g\ m^{-3}$) to distance travelled over the sea (km).

Period over sea		Relationship between chloride concentration and distance travelled over sea	r^2
Previous 24 h	0 to –24 h	$y = 0.0025\ x + 0.0995$	0.43
Preceding 24-h period	–24 to –48 h	$y = 0.0015\ x + 0.0994$	0.28
Previous 48 h	0 to –48 h	$y = 0011\ x + 0.0591$	0.39

6.1.5 Mass closure model for airborne particulate at roadside and background sites

549. Ninety-seven roadside and background samples obtained during the Traffic Management and Air Quality (TRAMAQ) study were quantitatively analysed for iron, calcium, sulphate, nitrate, chloride, elemental carbon and organic carbon. These analytes were chosen as representative of the major components of airborne particulate matter and factors were derived to calculate the mass of the component present.

● Iron: representative of suspended soil and road dust. Factors of 5.50 for the roadside samples and 9.00 for the background samples were chosen to account for other components of the dusts.

● Calcium: representative of construction dust. No difference was seen in the concentrations of calcium at the roadside and background sites. A factor of 4.30 was used to convert the mass of calcium to gypsum ($CaSO_4.2H_2O$).

● Sulphate: representative of ammonium sulphate, a major secondary component of airborne particulate. After subtracting a proportion of the

Figure 6.24 Relationships between chloride concentration and distance travelled over sea during various time periods.
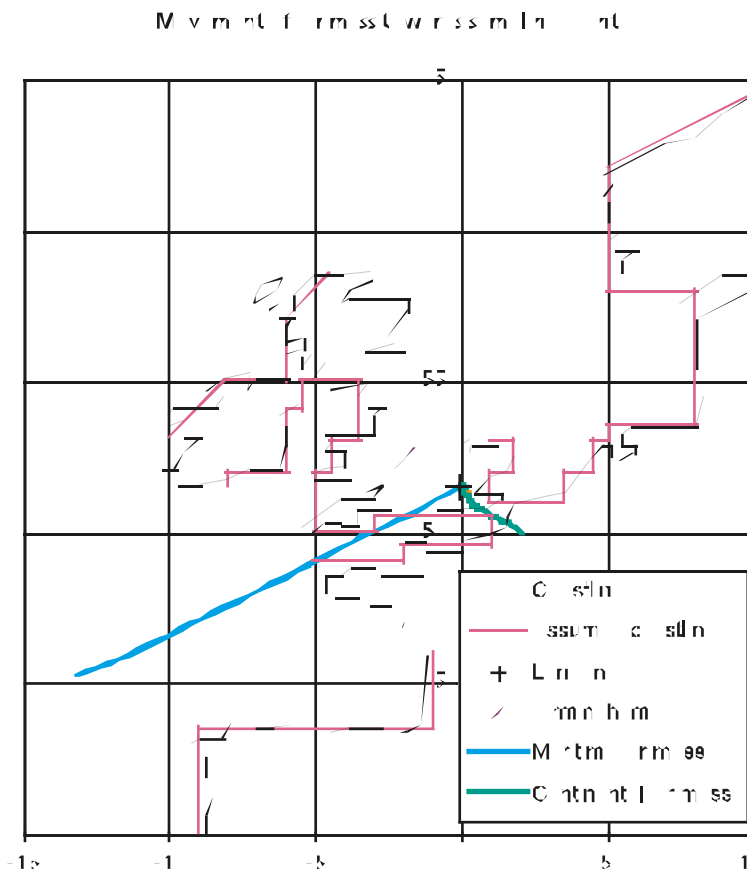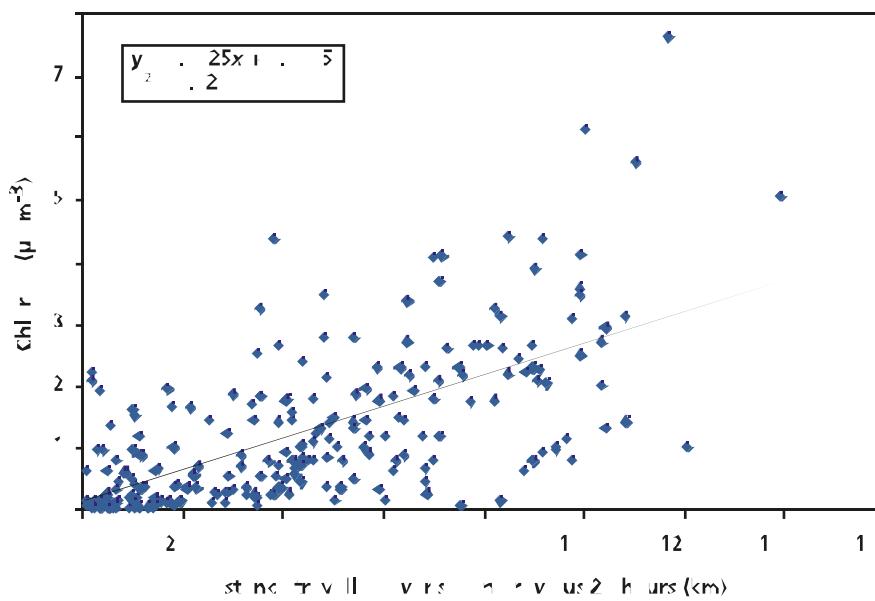

Figure 6.25 Concentration of chloride measured versus distance air mass travelled over sea in previous 24 h.

mass of calcium to allow for the presence of calcium sulphate, a factor of 1.38 was used to convert the mass of the remaining sulphate to ammonium sulphate.

● Nitrate: representative of ammonium nitrate and sodium nitrate, other major secondary components of airborne particulate. A factor of 1.29 was used to calculate the mass of NH_4NO_3 from the mass of the fine fraction of nitrate, and a factor of 1.38 was used to calculate the mass of $NaNO_3$ from the mass of the coarse fraction of nitrate.

● Chloride: representing marine aerosol. A factor of 1.65 was used to convert the mass of chloride to NaCl.

● Elemental carbon: resulting from combustion processes. It is a form of graphitic carbon and, therefore, a factor of 1.00 was used.

● Organic carbon: representing a combination of natural organic material and combustion products. Factors of 1.30 and 1.40 were used respectively to convert the roadside and background masses of organic carbon to the masses of organic compounds.

● Bound water: sulphates and nitrates are highly hygroscopic. A factor of 0.29 was used to calculate the mass of bound water from the masses of ammonium sulphate, ammonium nitrate and sodium nitrate.

This scheme is explained in more detail elsewhere (Harrison *et al*., 2003).

550. With the exception of the factors for iron, organic carbon and bound water, all the factors chosen were derived from the molecular weights of the compounds. The factors were used to calculate the total masses of PM_{10}, PM_{coarse} and $PM_{2.5}$ for each set of measured masses at the roadside and background sites and for the mass differences between the sites. Reduced major axis regression lines were fitted to the calculated and measured mass data and the factors chosen for iron, organic carbon and bound water were adjusted to obtain the most advantageous fitted line (gradient 1:1; intercept = 0).

551. The equations of the fitted lines are presented in Table 6.9 along with the squared correlation coefficients.

552. The calculated values of PM_{10} and PM_{coarse} at the roadside are plotted against the measured values in Figures 6.26 and 6.27, respectively. The fitted lines are good representations of the data. In the case of PM_{coarse} there is a greater scatter of the points about the line as would be expected from the lower value of the squared correlation coefficient.

553. The model, although simple, accounts for a large part of the variance in the mass concentration and encompasses the major components of the airborne particulate. The different factors chosen for iron and organic carbon at the roadside and background sites are compatible with there being higher concentrations of iron from mechanical wear and organic carbon from vehicle exhausts at the roadside sites. Trace metals and PAHs, discussed above, although

Table 6.9 Regression equations for lines fitted to the calculated and measured masses.

	Site	RMA regression equation	r^2	n
PM_{10}	Roadside	$y = 1.00\,x + 1.33$	0.92	97
PM_{coarse}	Roadside	$y = 1.00\,x + 0.19$	0.73	97
$PM_{2.5}$	Roadside	$y = 1.00\,x + 0.97$	0.93	97
PM_{10}	Background	$y = 0.99\,x + 2.50$	0.84	97
PM_{coarse}	Background	$y = 1.00\,x + 0.58$	0.61	97
$PM_{2.5}$	Background	$y = 1.01\,x + 1.52$	0.90	97
PM_{10}	Difference	$y = 1.08\,x - 0.96$	0.79	97
PM_{coarse}	Difference	$y = 0.99\,x - 0.11$	0.66	97
$PM_{2.5}$	Difference	$y = 1.19\,x - 1.52$	0.72	97

of potential importance in toxicological terms, are minor components, not analysed directly in the model. The PAHs comprise a component of the organic carbon, whereas the trace metals, unless soil-derived, are not accounted for explicitly, but represent only a very small proportion of the mass.

Figure 6.26 Relationship of calculated PM_{10} and weighed PM_{10} at roadside sites.
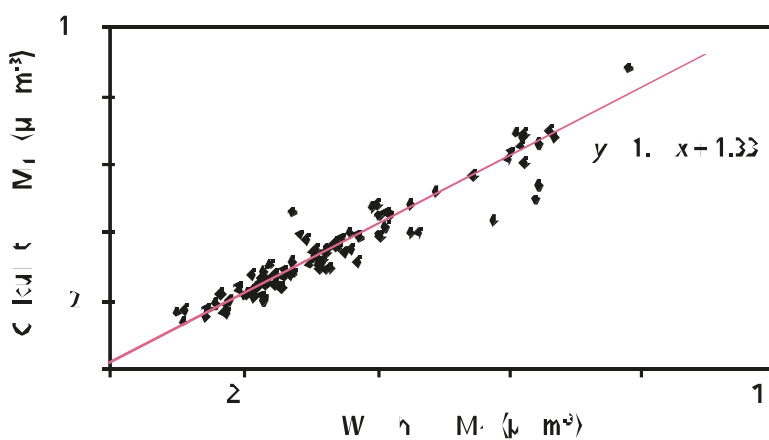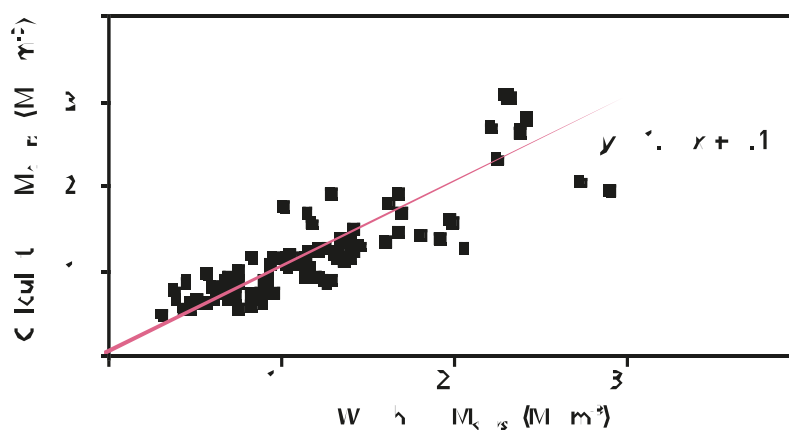

Figure 6.27 Relationship of calculated PM_{coarse} and weighed PM_{coarse} at roadside sites.

6.1.6 Chemical composition of roadside and urban background particles and the roadside increment

554. The mean chemical components of the airborne particulate calculated in the TRAMAQ study at the roadside and background sites are shown in Figures 6.28 to 6.31 for both coarse and fine PM fractions. The mean masses of each component are shown on the figures. Iron-rich dust is the largest component of both the roadside and background coarse PM, with a larger mass at the roadside sites. The masses of the other components are similar at both sites. Within the fine fraction, similar masses of ammonium nitrate, ammonium sulphate and bound water are present at both roadside and background sites, with the sum of organic compounds and elemental carbon making up two-thirds, and one-third of the of the total fine particulate at the roadside and background sites respectively.

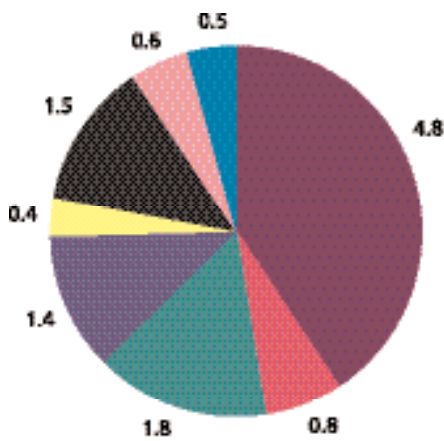**Figure 6.28** Chemical components ($\mu g\ m^{-3}$) at roadside sites – coarse fraction.

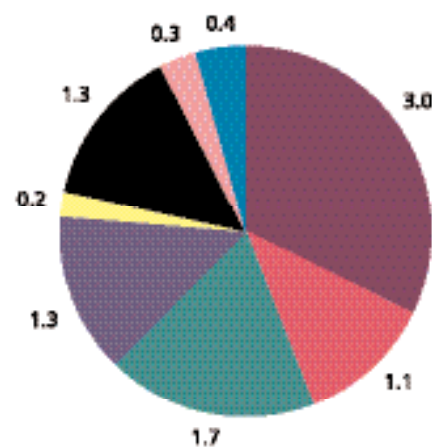**Figure 6.29** Chemical components ($\mu g\ m^{-3}$) at background sites – coarse fraction.

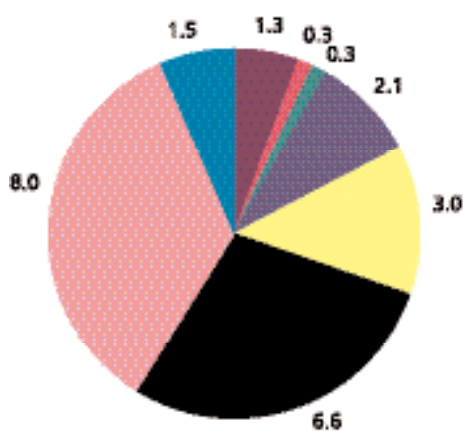**Figure 6.30** Chemical components ($\mu g\ m^{-3}$) at roadside sites – fine fraction.

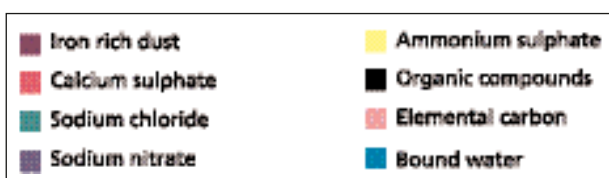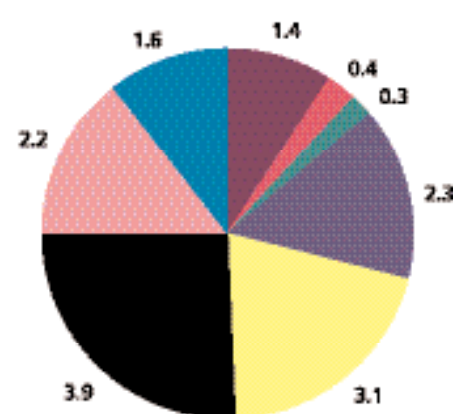**Figure 6.31** Chemical components ($\mu g\ m^{-3}$) at background sites – fine fraction.

Legend:
- Iron rich dust
- Calcium sulphate
- Sodium chloride
- Sodium nitrate
- Ammonium sulphate
- Organic compounds
- Elemental carbon
- Bound water

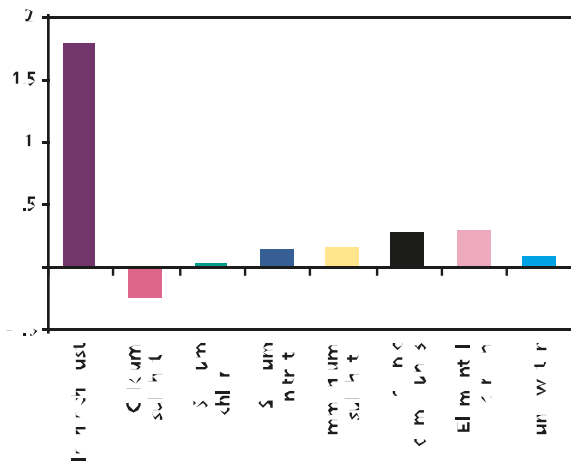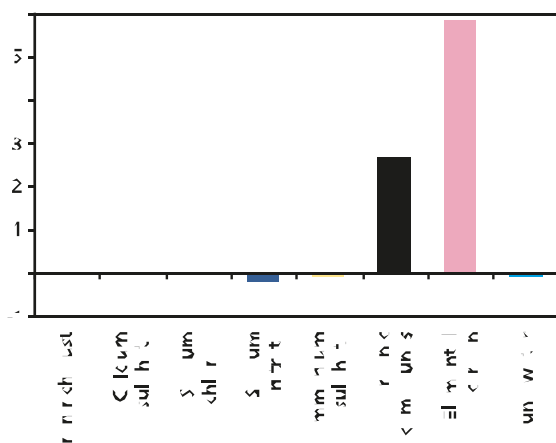**Figure 6.32** Roadside – background difference (µg m^{-3}) – coarse fraction.

**Figure 6.33** Roadside – background difference (µg m^{-3}) – fine fraction.

555. The differences between the calculated masses of the components of the airborne particulate matter in the coarse and fine fractions are shown in Figures 6.32 and 6.33. The difference in the coarse material is dominated by the iron-rich dust, with smaller contributions from sodium nitrate, ammonium sulphate, organic compounds and elemental carbon. Calcium sulphate was higher at the background sites than at the roadside sites. This may be due to localized sources of calcium sulphate, possibly from construction activities. In the fine fraction the difference between the roadside and background sites is dominated by the organic compounds and elemental carbon.

6.1.7 Apportionment of urban background PM$_{10}$ in Glasgow using mass-closure model

556. The mass closure model developed by Harrison *et al*. (2003) was applied to measurements of chemical composition of PM$_{10}$ at an urban background site in Glasgow. The 182 sets of measurements were nearly all from 24-h samples (although some samples were 48 h) collected between August 1999 and September 2000. In this work, measured nitrate could not be apportioned between ammonium or sodium nitrate, so a single multiplier of 1.33 was applied to the mass of nitrate measured, which is an average of the multipliers of 1.29

and 1.37 required to scale nitrate to ammonium and sodium nitrate, respectively. In addition, carbon was not apportioned between elemental and organic, and a single multiplier of 1.3 was used to give best agreement in regression of aggregated mass-closure mass on measured PM_{10}. Figure 6.34 shows the mean chemical apportionment for this site. The mean PM_{10} was 18.9 µg m^{-3} (gravimetric). Approximately one-third, on average – that is, ~7 µg m^{-3} (gravimetric) – of PM_{10} at this urban background site in Glasgow is constituted by primary mechanically (wind)-generated particles, that is, dust and sea salt. The relatively high proportion of sea salt is due to Glasgow's west coast location. Approximately one-third of the PM_{10} is due to secondary inorganic aerosol. The remaining one-third is carbonaceous aerosol, although this cannot be apportioned between primary elemental carbon from local sources and organic carbon either from local sources or as longer range secondary organic aerosol.

Figure 6.34 Apportionment of urban background PM_{10} in Glasgow using the mass closure model of Harrison *et al*. (2003). Proportions are means of *n* = 182 samples.
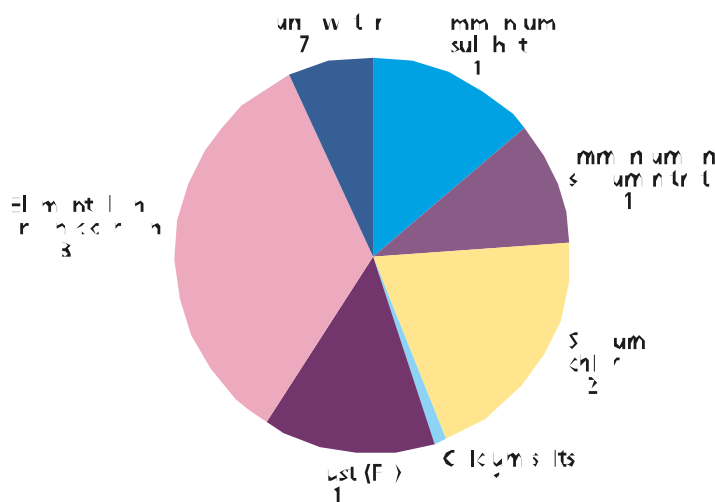
6.2 Spatial distribution of PM

6.2.1 Spatial distribution of PM_{10} within and between Edinburgh and Glasgow

557.	Measurements of daily PM_{10} at two separate urban centre sites in Edinburgh and at two separate urban centre sites in Glasgow provide evidence of a reasonably strong spatial correlation in background PM_{10} for both cities, see Figures 6.35 and 6.36 (*r* = 0.64 and *r* = 0.56 for Edinburgh and Glasgow, respectively).

558.	The value of the correlation coefficient (*r* = 0.50) between the mean of the PM_{10} from the two sites in Edinburgh and the mean of the PM_{10} from the two sites in Glasgow for almost 1 year's measurements is almost as strong as the correlation in PM_{10} within each city (Figure 6.37). Although these two cities are separated by only ~80 km, these data indicate that for roughly comparable cities in the UK, a significant proportion of variability in PM_{10} is controlled by regional-scale sources and synoptic meteorology.